Geophys. J. Int. (2006) **165,** 272–278 doi: 10.1111/j.1365-246X.2006.02890.x

Fault creep growth model and its relationship with occurrence of earthquakes

Zuan Chen and Wuming Bai

Institute of Geology and Geophysics, Chinese Academy of Sciences, Beijing 100029, *China. E-mail: zachen@mail.igcas.ac.cn*

Accepted 2005 December 16. Received 2005 December 8; in original form 2004 December 7

SUMMARY

A fault model is used to analyse creep growth process of microcracks in damage zone near the tips of fault by means of the rheology fracture mechanics. When microcracks in the zone link each other and their deformation quickly intensifies, it means that an earthquake is taking place to a certain degree. The relationships among some key parameters that are correlated to the growth of microcracks are analysed theoretically. These parameters include failure time of fault, number of microcracks in unit area, stresses field, yield strength and rheological properties of medium. The results indicate that the model proposed here is reasonable to describe the pregnant process of an earthquake. In the meantime, this research shows that, with the results of *in situ* surveys and lab experiments, it is possible to estimate the time span for a fault expanding.

Key words: creep, earthquake, fault, growth, microcrack, model.

1 INTRODUCTION

Faults can have close relationship with earthquakes. Faults may range in length from a few meters to many kilometres. In the field, geologists commonly find many discontinuity planes in rock matrix, which they interpret as faults. The presence of such faults indicates that, at some time in the past, a relative movement took place along them. We know that such movement can be either slow slip, which produces no ground shaking, or sudden rupture, which results in perceptible vibrations—an earthquake. A lot of work has been done to analyse the causes and processes of fault slip (Cox & Scholz 1988; Lloyd & Knipe 1991; Lockner *et al.* 1991; Cowie & Scholz 1992; Sleep & Blanpied 1992).

Studies of faulting conventionally characterize faults as discrete planar surfaces, which accommodate slip. Observations of naturally and experimentally formed faults show difference with this idealization. While discrete surfaces are produced, a more complex deformation also occurs within a region of material surrounding these surfaces. Studies on the deformation of damaged zone belong to a fundamental subject. However, a systematic survey and studies on model of the forming process of damage zones around the faults are still lacking (Scholz *et al.* 1993).

We cannot treat fault growth process by a simple elastic crack model, because such model contains a stress singularity at the crack tip, which is physically unreasonable. Instead, we should use an elastic-plastic fracture mechanics model, which includes a breakdown zone involving inelastic deformation in a region surrounding the fault tips. The Dugdale–Barenblatt model is the simplest model of this type and has the advantage of an analytical solution (Dugdale 1960; Barenblatt 1962). The application of this model to faulting is described in detail by Cowie & Scholz (1992). A cohesion zone model developed by them can be used to describe fault growth as a physical process, and this model is consistent with observed results in this growing process.

The purpose of this paper is to put forward a rheological growing model of microcracks in damage zone surrounding the tip of fault and to describe the pregnant process of earthquake with an analytical method. The relationship among some key parameters that are correlated to the growth of microcracks is analysed theoretically. The parameters include failure time of fault, initial size and orientations of microcracks, number of microcracks in unit area, stresses field, yield strength, and rheological properties of medium. The analyzing method employed here could be conveniently extended to the estimation of the time of an earthquake occurrence.

2 THE PRELIMINARY WORK

We consider a strike-slip fault with length L_f loaded in remote field stress σ_1 and σ_3 (positive for extension and negative for compression). The angle between the fault and principal stress σ_1 is assumed as ψ (as shown in Fig. 1). It is obvious that the primary mechanics problem illustrated in Fig. 1 is equivalent with that on the left of equal sign shown in Fig. 2(a). In the equivalent problem, a friction force exists on the surface of the fault. The normal stress σ and shear stress τ have the following relationships with principle stresses σ_1 and σ_3, respectively,

$$\begin{aligned} \tau &= \frac{\sigma_3 - \sigma_1}{2} \sin 2\psi \\ \sigma &= \frac{\sigma_3 + \sigma_1}{2} + \frac{\sigma_3 - \sigma_1}{2} \cos 2\psi, \end{aligned} \tag{1}$$

where τ is shear stress and σ is normal stress on the fault.

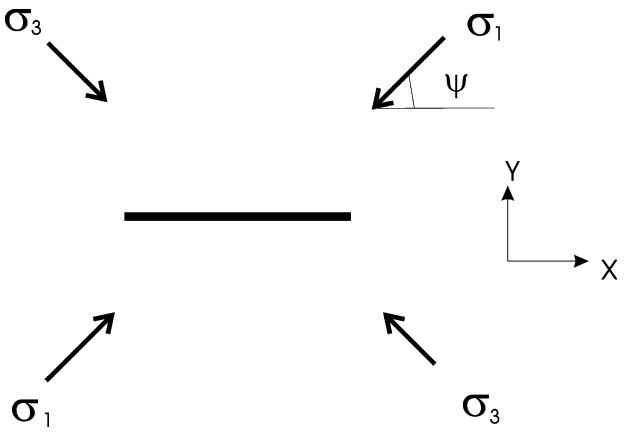

Figure 1. A fault under tectonic stresses.

The original problem thus can be decomposed into two problems, that is, a shear problem with friction force on surface of fault and an axial compression problem without fault, illustrated in Fig. 2(a). In Fig. 2(a), the first problem on the right side of the equal sign may further be superposition of two problems, one is a pure shear problem without friction force on surface of fault, and the other is a shear problem without fault, as illustrated in Fig. 2(b). In Fig. 2(b), the first problem on the right side of the equal sign is a typical shear fracture mode (mode Π), and the elastic stresses at the tip of the crack are given by (Miannay 1998)

$$\sigma_{xx}(r,\theta) = -\frac{K_\Pi}{\sqrt{2\pi r}}\left(2+\cos\frac{\theta}{2}\cos\frac{3\theta}{2}\right)\sin\frac{\theta}{2}$$
$$\sigma_{yy}(r,\theta) = \frac{K_\Pi}{\sqrt{2\pi r}}\sin\frac{\theta}{2}\cos\frac{\theta}{2}\cos\frac{3\theta}{2}$$
$$\sigma_{xy}(r,\theta) = \frac{K_\Pi}{\sqrt{2\pi r}}\left(1-\sin\frac{\theta}{2}\sin\frac{3\theta}{2}\right)\cos\frac{\theta}{2}, \qquad (2)$$

where r and θ are polar coordinate centred at the tip of fault, and

$$K_\Pi = \sqrt{\pi L_f}(\tau+\mu\sigma) \qquad (\text{if } |\tau| > |\mu\sigma|) \qquad (3)$$

where μ is friction coefficient, L_f is the length of fault and K_Π is the stress intensity factor.

In these formulas, the stresses at the fault tip are singular ($r \to 0$), which correspond to the elastic solution of the problem. According to the superposition theorem, the elastic stresses along the fault plane near crack tip for primary problem shall be

$$\sigma_{xx}(r,0) = 0.0$$
$$\sigma_{yy}(r,0) = \sigma$$
$$\sigma_{xy}(r,0) = \frac{K_\Pi}{\sqrt{2\pi r}} - \mu\sigma. \qquad (4)$$

If we assume this problem as a plane strain problem, then

$$\sigma_{zz}(r,0) = \nu(\sigma_{xx}(r,0)+\sigma_{yy}(r,0)) = \nu\sigma, \qquad (5)$$

where ν is Poisson ratio.

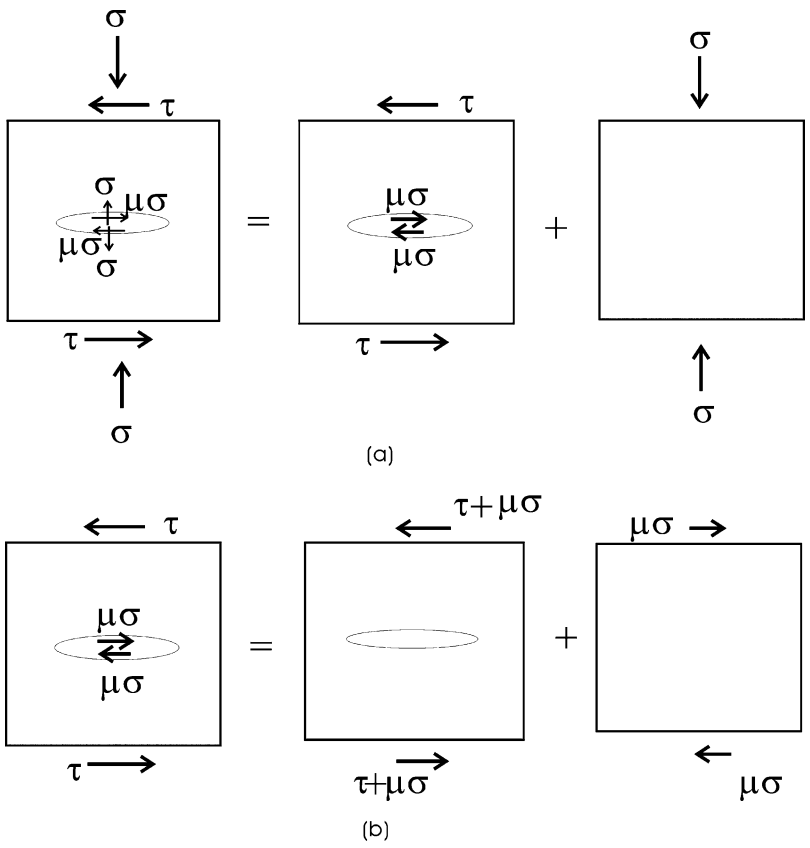

Figure 2. Equivalent problems sketch.

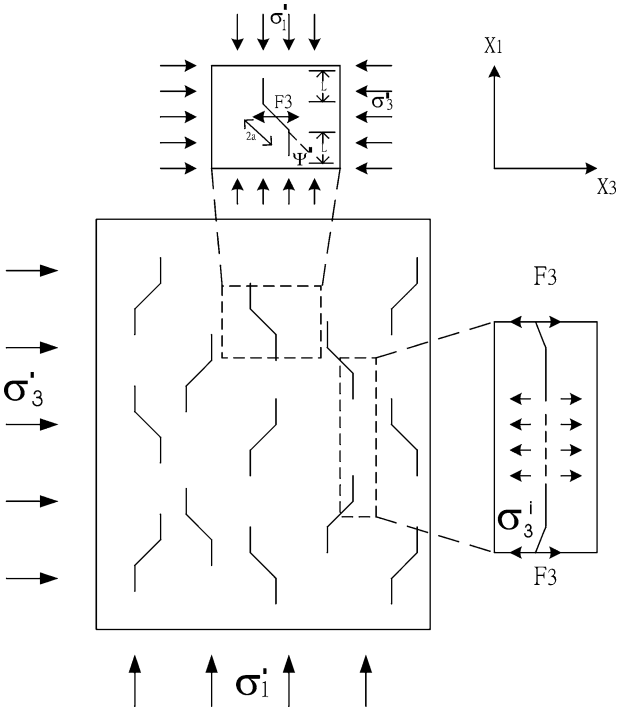

Figure 3. Model of extending microcracks.

If we take the plastic deformation of rocks into account, then when stresses exceed the yield strength, the medium around the tip of fault will yield. The length of the yield region along fault plane is defined as r_b, which is determined by Mises yield criterion.

Mises yield criterion (Han & Reddy 1999) is expressed as follows:

$$\sqrt{\frac{1}{2}\left[(\sigma_{11}-\sigma_{22})^2+(\sigma_{22}-\sigma_{33})^2+(\sigma_{33}-\sigma_{11})^2\right]}=\sigma_s, \tag{6}$$

where σ_s is yield strength of single axial compressive stress; σ_{11}, σ_{22} and σ_{33} are principle stresses, which may be determined by σ_{xx}, σ_{yy}, σ_{zz} and σ_{xy} (Jaeger & Cook 1976).

Combining eqs (4), (5) and (6) , we may obtain the length $r_b$of the yield region along fault plane, as indicated in

$$r_b=\frac{K_\Pi^2}{2\pi\left[\sqrt{\frac{1}{3}\left[\sigma_s^2-(1-\nu+\nu^2)\sigma^2\right]}+\mu\sigma\right]^2}. \tag{7}$$

When $\sigma=0$,

$$r_b=\frac{3K_\Pi^2}{2\pi\sigma_s^2}, \tag{8}$$

which is the result of pure shear mode Π (Miannay 1998).

3 THEORETICAL MODEL

In the paper, we intend to build up an earthquake pregnant model and to analyse the creep growth process of the faults. In the model, the faults are treated as a shear cracks that have friction forces acting on their inner sides, as stated above. The extension of faults is through a complex fracturing process.

First, we suppose that a fault extend on its plane in the yield zone. Although the narrow strip of extending seems as a line in macroscopic view, it contains a lot of microcracks on microscopic level due to yield or dilatancy. As a matter of fact, according to fracture mechanics, an array of tensile microcracks is generated in the yield zone near the fault tips, with orientations being consistent with the maximum compressive stress direction. Continued shearing results in the development of a complex mesh of fracture concentrated within this brittle process zone, which eventually breaks down to form a thoroughgoing fault.

Secondly, we propose a microcrack model, in which an array of microcracks with the same shape and initial size are distributed evenly along the fault plane in the yield zone near fault tips, as illustrated in Fig. 3. The medium in the yield zone containing many microcracks is viscoplastic, while the rock material around the microcracks exhibit viscoelasticity. Under triaxial stresses, the microcracks will extend time-dependently on the direction of the maximum compressive stress. Due to rheological properties of the rocks around the microcracks, those microcracks will gradually grow with time until they link each other to form a new fault.

The stresses in yield zone at the tip of the fault along fault plane shall be constant, and are expressed by

$$\begin{aligned}\sigma_{xx}&=0\\ o_{yy}&=\sigma\\ \sigma_{xy}&=\frac{K_\Pi}{\sqrt{2\pi r_b}}-\mu\sigma.\end{aligned} \tag{9}$$

The local field the stress will create a shear stress τ' and a normal stress σ' on surface of initial microcrack. The sliding of microcracks (resisted by the frictional force, with friction coefficient μ), opens the mouth of each wing crack. The wedging can be deemed to be a result of the force F_3 that is parallel to X and acts at the midpoint of the microcrack (Ashby & Sammis 1990; Chen 2003). Stress σ' and τ' are given by

$$\begin{aligned}\tau'&=\frac{\sigma_2'-\sigma_1'}{2}\sin 2\psi'\\ \sigma'&=\frac{\sigma_1'+\sigma_2'}{2}+\frac{\sigma_2'-\sigma_1'}{2}\cos 2\psi'\end{aligned} \tag{10}$$

$$\begin{aligned}\sigma_1'&=\frac{\sigma}{2}+\frac{1}{2}\sqrt{\sigma^2+4\left(\frac{K_\Pi}{\sqrt{2\pi r_b}}-\mu\sigma\right)^2}\\ \sigma_2'&=\frac{\sigma}{2}-\frac{1}{2}\sqrt{\sigma^2+4\left(\frac{K_\Pi}{\sqrt{2\pi r_b}}-\mu\sigma\right)^2},\end{aligned} \tag{11}$$

where σ'_1 and σ'_2 are principle stresses in yield region along fault plane, and the angle between the initial microcrack and principal stress σ'_1 is assumed as ψ' (as shown in Fig. 3).

F_3 may be expressed by

$$F_3=(\tau'+\mu'\sigma')2a\sin\psi'. \tag{12}$$

Also there is an average internal stress, acting on the wing cracks that describes the interaction among cracks:

$$\sigma_2^i=\frac{F_3}{S-2(L+a\cos\psi')}, \tag{13}$$

where S is the distance between the central points of wing cracks, 2a is the length of the microcrack and L is the extending length of the microcrack. If the number of microcracks in unit area is N, the relation between S and N is

$$S=\frac{1}{\sqrt{N}}. \tag{14}$$

Therefore, the stress intensity factor at tips of wing cracks is given by (Ashby & Sammis 1990; Chen 2003)

$$K_{\mathrm{I}} = \frac{F_3}{\sqrt{\pi(L+\beta a)}} + (\sigma_2' + \sigma_2^i)\sqrt{\pi L}. \tag{15}$$

4 CALCULATING ANALYSIS

We have previously analysed the creep growth process of microcracks in the above model, and obtained the relationship between the microcrack growth velocity and various factors such as principal stresses, initial length of microcrack and so on (Chen 2003). Some useful contents will be mentioned again in detail as follows so as to make the present task easy to understand.

Under the isothermal condition, the appropriate statement of the global conservation of energy for extension of cracks in viscoelastic media (Christensen 1982) is given by

$$\frac{dU}{dt} + \frac{dDp}{dt} + \frac{dSe}{dt} = 0, \tag{16}$$

where U is the elastic energy in infinite plate contained one crack, Dp is the dissipation energy due to rheology of the medium and S_e is surface energy. Eq. (16) may also be written as

$$\frac{dU}{dL} + \frac{dDp}{dL} + \frac{dSe}{dL} = 0. \tag{17}$$

The expression for the energy change rate (Jaeger and Cook, 1976) may be used for the model mentioned above. When neglecting K_{II} (which is referred to type two stress intensity factor at tips of microcracks herein and is different from eq. 3):

$$\frac{dU}{dL} = -\frac{2K_{\mathrm{I}}^2(1-\nu^2)}{E}, \tag{18}$$

where ν is the Poisson ratio and E represents the Young 's modulus.

To make the analysis easier, we suppose the extension of microcracks will take place step by step. Accordingly, the wing of microcrack begins from initial state ($L = 0$), through the time period $T(0)$, to grow to a length L and then stop; then after another time period $T(L)$, the microcrack continues to grow to a new length L and stops again. Furthermore, there exists a critical length L_0. When L is larger then L_0, $T(L)$ is equal to zero, which means microcrack growth will accelerate until failure. $T(L)$ is the time period from the stop of the last microcrack extension up to the start of the next microcrack extension.

Considering the actual process of microcrack extension described above, the stress around tip of microcracks will be constant in duration with microcrack growth stopping temporarily, in accordance with the correspondence principle. The stress formula for a type I crack is

$$\sigma_{ij} = \frac{K_{\mathrm{I}}}{\sqrt{r}} f_{ij}(\theta), \tag{19}$$

where r and θ are polar coordinates, and the origin is at tip of the wing crack (which will move with extension of the crack). σ_{ij} is stress tensor and K_{I} is stress intensity factor. $f_{ij}(\theta)$ is a function depending on loading type.

The viscoelastic constitutive equation for creep may be written as follows:

$$\begin{aligned} e_{ij} &= S_{ij} D(t) \\ e_v &= pK(t) \\ e_v &= \varepsilon_{ii}/3 \\ p &= \sigma_{ii}/3 \\ e_{ij} &= \varepsilon_{ij} - \varepsilon_0 \\ S_{ij} &= \sigma_{ij} - p\delta_{ij}, \end{aligned} \tag{20}$$

where $D(t)$ and $K(t)$ are the deviatoric strain creep compliance and the volume strain creep compliance, respectively. σ_{ij} and ε_{ij} are the stress tensor and strain tensor, respectively, in a coordinate system that moves with the crack extension. The origin of the coordinate system is again at the tip of cracks. While S_{ij} is the deviatoric stress tensor, p is the hydrostatic stress, e_{ij} is the deviatoric strain tensor and e_v is the volumetric strain.

Dissipative energy Q at some point of the medium may be calculated as

$$Q = \int_0^T \sigma_{ij}\dot{\varepsilon}_{ij}\, d\zeta, \tag{21}$$

where time T counts from the halting of crack growth. It is assumed that the dissipation of energy is caused by stresses singularity at tip of cracks.

Taking a circle around tip of crack, the total dissipative energy may be calculated as follows:

$$\begin{aligned} dDp &= -\int_0^{dL}\int_{-\pi}^{\pi} Q\pi\, d\theta\, dr \\ &= -\pi K_{\mathrm{I}}^2[G(T) - G(0)]\, dL \end{aligned} \tag{22}$$

$$\frac{dDp}{dL} = -\pi K_{\mathrm{I}}^2[G(T) - G(0)] \tag{23}$$

$$G(T) = \frac{2}{3}[(1-\nu)D(T) + 2(1+\nu)K(T)], \tag{24}$$

where the negative signs indicate loss of energy.

The surface energy is

$$\frac{dSe}{dL} = 2\eta, \tag{25}$$

where η represents surface energy per unit area.

Combining eqs (18), (23), (25) and (17), the following formula can be derived

$$G(T) = \frac{2}{\pi K_{\mathrm{I}}^2}\left[\eta - \frac{K_{\mathrm{I}}^2(1-\nu^2)}{E}\right] + G(0), \tag{26}$$

Eq. (26) must be satisfied by $T(L)$.

If the viscoelastic creep compliance is taken as

$$\begin{aligned} D(t) &= \beta_s \ln(1+\alpha_0 t) \\ K(t) &= 0, \end{aligned} \tag{27}$$

where β_s and α_0 are creep coefficients, which determine the rate of rock deformation in creeping process. This creep compliance form is also called logarithmic creep (Miannay 2001). Combining (24), (26) and (27), the following equation can be found:

$$T(L) = \left\{ \exp\left[\frac{3}{\pi\beta_s(1-\nu)}\left(\frac{\eta}{K_{\mathrm{I}}^2} - \frac{1-\nu^2}{E}\right)\right] - 1\right\}/\alpha_0. \tag{28}$$

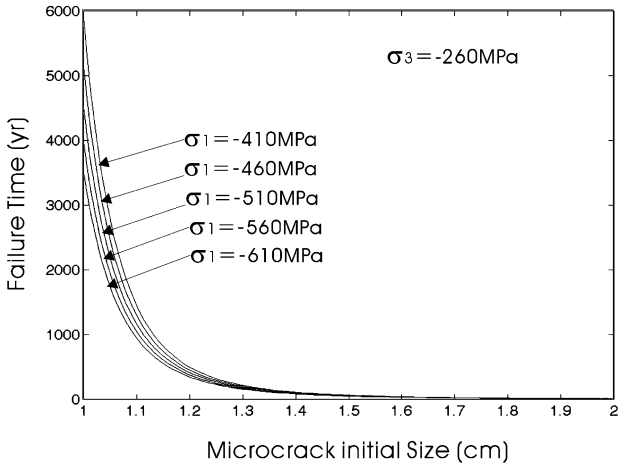

Figure 4. Relationship between the failure time and the initial microcrack size for different principle stresses: $\sigma_3 = -200$ MPa; $L_f = 50$ km; $\psi = \pi/3$; $\mu = 0.5$; $\nu = 0.25$; $\sigma_s = 350$ MPa; $\psi' = \pi/4$; $N = 0.308\,\mathrm{m}^{-2}$; $\eta = 50\,000$ MPa; $E = 50\,000$ MPa; $\beta_s = 1\ (\mathrm{MPa})^{-1}$; $\alpha_0 = 43.8$ yr.

Take t_r as the failure time, which stands for the time period from microcracks starting to extend to the moment of their interconnection. Therefore,

$$t_r = \int_0^{L_0} T(L)\,dL. \tag{29}$$

Eq. (29) may be calculated numerically with Gauss formula as follows:

$$t_r = \sum_{i=1}^{n} H_i T(L_i), \tag{30}$$

where $H_i (i = 1 \sim n)$ is weight factor, and $L_i (i = 1 \sim n)$ is a number between 0 and L_0.

5 COMPUTING RESULTS

The time t_r may also be considered to be the pregnant time for an earthquake from its definition thereof and is related to many factors such as tectonic stresses, yield strength, initial size of microcracks, crack number in unit area, fracture and rheological parameters.

(1) The influence of tectonic stress.
The field stresses determine the size of yield zone and the local stresses in the yield zone. The stresses in the yield zone have an influence on the time for the microcracks to interconnect, or the time to fracture. The normal stress on fault plane is determined by the direction and the magnitude of the principle tectonic stresses. It reduces the yield radius and prevent the microcracks around fault tips from propagating. The relationship between the failure time and the initial microcrack size for different principle stresses is shown in Fig. 4. As it indicates, the failure time reduces as the difference stress increases.

(2) The influence of yield strength.
The value of yield strength determines the level of stresses in the yield zone, and influence the failure time. Yield radius r_b reduces with the increases of yield strength. Based on experimental results in lab, we take 350 MPa as the yield stress for granite, and 300 MPa for marble. The yield radius r_b ranges from 5 m to a few hundred metres. Fig. 5 shows the relationship between the failure time and the initial microcrack size for different yield strengths. As is indicated in the figure, the failure time reduces with the increase of yield strength.

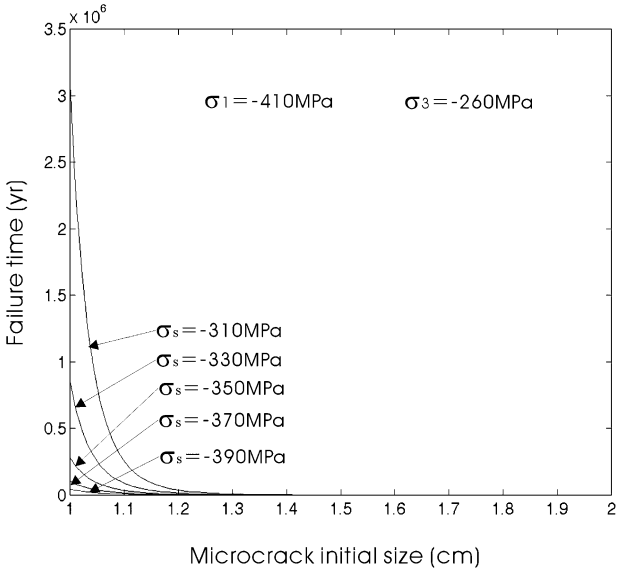

Figure 5. Relationship between the failure time and the initial microcrack size for different yield strengths: $\sigma_1 = -410$ MPa; $\sigma_3 = -200$ MPa; $L_f = 50$ km; $\psi = \pi/3$; $\mu = 0.5$; $\nu = 0.25$; $\psi' = \pi/4$; $N = 0.308\,\mathrm{m}^{-2}$; $\eta = 50\,000$ MPa; $E = 50\,000$ MPa; $\beta_s = 1\ (\mathrm{MPa})^{-1}$; $\alpha_0 = 43.8$ yr.

(3) The influence of the number of microcracks in unit area.
As shown in eq. (14), the distance between two microcracks along fault plane reduces with the increase of the number of microcracks in unit area; therefore the time before the final breakthrough will be shorter. Fig. 6 shows the relationship between the failure time and the initial microcrack size for different microcrack number in unit area.

(4) The influence of surface energy in unit area.
The value of surface energy in unit area reflects the fracture strength of medium around microcracks. If surface energy in unit area is relatively large, the energy dissipation will take a comparatively

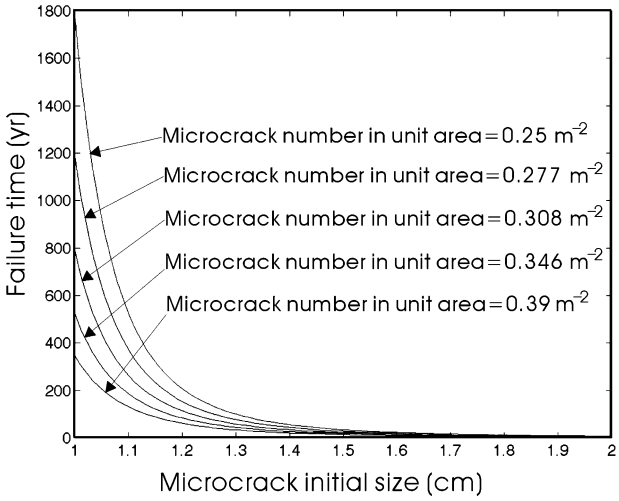

Figure 6. Relationship between the failure time and the initial microcrack size for different microcrack number in unit area: $\sigma_1 = -410$ MPa; $\sigma_3 = -200$ MPa; $L_f = 50$ km; $\psi = \pi/3$; $\mu = 0.5$; $\nu = 0.25$; $\sigma_s = 350$ MPa; $\psi' = \pi/4$; $\eta = 50\,000$ MPa; $E = 50\,000$ MPa; $\beta_s = 1\ (\mathrm{MPa})^{-1}$; $\alpha_0 = 43.8$ yr.

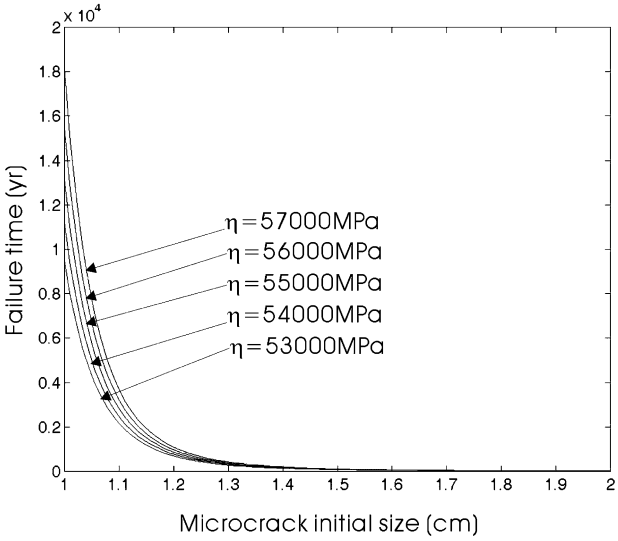

Figure 7. Relationship between the failure time and the initial microcrack size for different surface energy in unit area of medium around microcracks: $\sigma_1 = -410$ MPa; $\sigma_3 = -200$ MPa; $L_f = 50$ km; $\psi = \pi/3$; $\mu = 0.5$; $\nu = 0.25$; $\sigma_s = 350$ MPa; $\psi' = \pi/4$; $N = 0.308\,\mathrm{m}^{-2}$; $E = 50\,000$ MPa; $\beta_s = 1$ $(\mathrm{MPa})^{-1}$; $\alpha_0 = 43.8$ yr.

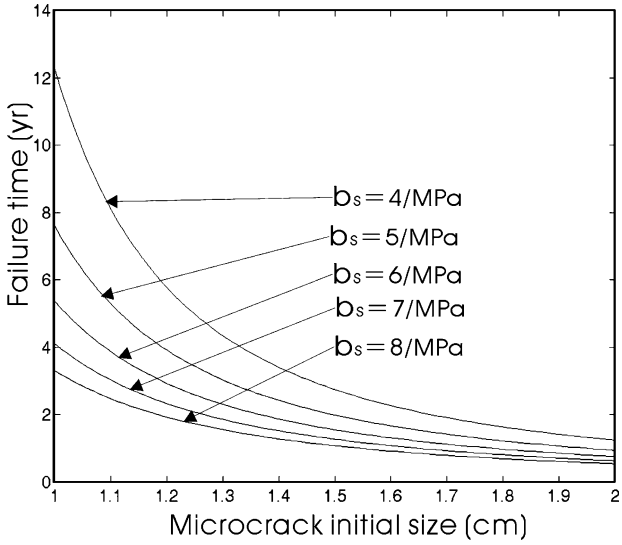

Figure 9. relationship between the failure time and the initial microcrack size for different rheological parameter b_s of medium around microcracks: $\sigma_1 = -410$ MPa; $\sigma_3 = -200$ MPa; $L_f = 50$ km; $\psi = \pi/3$; $\mu = 0.5$; $\nu = 0.25$; $\sigma_s = 350$ MPa; $\psi' = \pi/4$; $N = 0.308\,\mathrm{m}^{-2}$; $\eta = 50\,000$ MPa; $E = 50\,000$ MPa; $\alpha_0 = 43.8$ yr.

longer time until the final breakthrough of the microcracks. Fig. 7 indicates the relationship between the failure time and the initial microcrack size for different surface energy in unit area.

(5) The influence of rheological parameters.

The rheological property of rock is another important factor that influences the final breakingthrough time of the microcracks. The equation that figures the viscoelastic property of rock around cracks is taken in logarithm form in the paper, which implies that the energy dissipation will not cease until the microcracks interconnect with each other. Fig. 8 and Fig. 9, respectively, indicate the relationship between the failure time and the initial microcrack size for different rheological parameter a_0 and b_s.

(6) The influence of microcrack size.

Besides the number of microcracks in unit area, the initial size of microcrack is another parameter that affects the failure time. As illustrated above (Figs 4–9), the initial length of microcracks ranges from several millimetres to several centimetres, and the relative failure time ranges from millions of years to a few months.

(7) The influence of initial fault length.

The initial length of fault mainly determines the size of the yield area or yield radius r_b. Although the initial length of fault does not affect the expansion time of the fault directly, it does have a relationship with the scale of an earthquake. The longer the initial fault, the larger the earthquake, if the earthquake is due to occur.

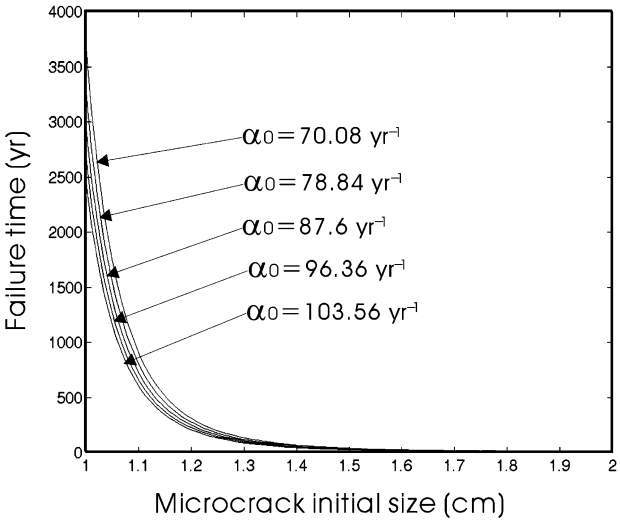

Figure 8. Relationship between the failure time and the initial microcrack size for different rheological parameter a_0 of medium around microcracks: $\sigma_1 = -410$ MPa; $\sigma_3 = -200$ MPa; $L_f = 50$ km; $\psi = \pi/3$; $\mu = 0.5$; $\nu = 0.25$; $\sigma_s = 350$ MPa; $\psi' = \pi/4$; $N = 0.308\,\mathrm{m}^{-2}$; $\eta = 50\,000$ MPa; $E = 50\,000$ MPa; $\beta_s = 1$ $(\mathrm{MPa})^{-1}$.

6 DISCUSSION

In the Vermilye & Scholz (1998) study, microfractures in damaged zone show logarithmic density increases with proximity to the fault, maximum density of which is independent of fault length, and their oritentions can be used to infer the direction of propagation of the fault plane. The analysis in this paper also shows that the initial microcrack density is correlated to the yield strength of rock, which is a constitutive property and is independent of fault length. To simplify the mathematical treatment, it is assumed that the microcracks in the proposed model have an even distribution.

Cowie & Scholz (1992) and Scholz *et al.* (1993) examined field data of slip on discrete faults with finite length and found that the slip distribution is tapered and is self-similar. Making the assumption that the geologic slip distribution is similar to that in a single event, they conclude that the size of the breakdown zone scales with fault length, which implies that fracture energy G, the energy loss per

unit fault area, is proportional to fault length. Estimates of G from laboratory experiments of shear fracture development in intact samples are approximately 10^4 J m^{-2}. However, much smaller values of G (10–10^2 J m^{-2}) have been obtained from experiments using samples with an artificially introduced slip surface. In contrast, estimates of G from earthquakes are in the range 10^6–10^7 J m^{-2}. In the creep growth model proposed in the paper, a part of energy is dissipated due to the creep growth of the microcracks, and the fracture energy G is then reduced. Therefore, the intensity of the earthquake deduced from our model might be smaller than that from a static mechanics analysis.

In the fault creep growth model proposed in the paper, even if the tectonic stresses keep constant, the microcracks in the zone near the tip of the fault still extends unceasingly due to the rheology property of the medium around the microcracks. Except for the initial size of microcracks, microcrack number in unit area, tectonic stresses and yield strength, the surface energy per unit area and the creep coefficients in formula (27) are important parameters, which have influences on the growth progress of microcrack. The surface energy per unit area is also an elastic strain energy release rate at crack propagation in elastic fracture mechanics. The creep coefficients in formula (27) may be obtained from a creep test in laboratory on a perfect rock sample without microcracks.

7 CONCLUSION

The progressive failure leading to collapse of faults has been studied numerically and experimentally (Lockner & Moore 1992; Tang *et al.* 1993; Tang 1997; Tang & Kaiser 1998; Tang *et al.* 2003). Being different from those studies, this paper considers the fault sliding as a time-dependent process, then reaches the following results.

First, the creep growth of microcracks in yield area surrounding the tip of a fault is a possible mechanism that could ultimately lead to expansion of a fault. The pregnant time of fault rupture can be expressed by t_r that is the time span between the initial state of microcracks and the final interconnection among them. The breakthrough of microcracks can cause fault sliding and lead to an earthquake.

Secondly, the initial microcrack length and microcrack number in unit area in yield zone around fault tips are key elements to control the creep time to failure or the occurrence of foreshock, although they cannot be determined theoretically at present. Failure or breakthrough time of microcracks less than 5-mm long will take about millions of years; meanwhile, to the larger microcracks, that is, 20-mm long or larger, the failure time might be only a few years. If it is possible to measure the size of microcracks in field, it is also possible to predict the occurrence of earthquakes.

Finally, the interconnection of microcracks will ultimately lead to the sliding of faults. According to the analysis above, the extent of fault growth is the yield radius r_b. However, due to dynamic mechanic effect, when the yield zone is broken through, there might leading occur new brittle rupture outside the yield zone, thus leading to a larger earthquake.

In summary, the intend of this paper is to quantitatively analyse the creep process of microfracturing in yield zone around the fault tips. A simple creep growth model of microcracks in yield zone under field stresses is proposed to deepen the understanding of the pregnant process of an earthquake. It has in substance answered a question, that is, when we have the knowledge of the initial size, initial density and orientations of microcracks and field stresses, we might roughly estimate the time when the microcracks in yield zone around fault tips interconnect with each other during creep process, or when an earthquake to a certain degree will happen.

ACKNOWLEDGMENTS

Our appreciation in advance shall be given to the editors and reviewers for their valuable comments. This work is supported by Chinese NSF (10032040 and 40574017).

REFERENCES

Ashby, M.F. & Sammis, C.G., 1990. The damage mechanics of brittle solid in compression, *Pure appl. Geophys.,* **133,** 489–521.

Barenblatt, G.I., 1962. The mathematical theory of equilibrium cracks brittle fracture, *Adv. Appl. Mech.,* **7,** 55–80.

Chen, Z., 2003. Analysis of a microcrack model and constitutive equation for time-dependent dilatancy of rock, *Geophys. J. Int.,* **155,** 601–608.

Cowie, P.A. & Scholz, C.H., 1992. Physical explanation for the displacement-length relationship of faults using a post-yield fracture mechanic model, *J. Struct. Geol.,* **14,** 1133–1148.

Cox, S.J.D. & Scholz, C.H., 1988. Rupture initiation in shear fracture of rocks: An experimental study, *J. geophys. Res.,* **93,** 3307–3320.

Christensen, R.M., 1982. *Theory of Viscoelasticity—An Introduction*, 2nd edn, Academic, New York.

Dugdale, D.S., 1960. Yielding of steel sheets containing slits, *Mech. Phys. Solids,* **8,** 100–115.

Griffith, A.A., 1924. Theory of rupture, in: *Proc. Ist Int. Congress Applied Mechanics*, Delft, the Netherlands, pp. 55–63.

Han, W. & Reddy, B.D., 1999. *Plasticity*, Springer-Verlag, New York.

Jaeger, J.C. & Cook, N.G.W., 1976. *Fundamentals of Fracture Mechanics*, 2nd edn, Chapman and Hall, London.

Lloyd, G.E. & Knipe, R.J., 1991. Deformation mechanisms accommodating faulting of quartzite under upper crustal condition, *J. Struct. Geol.,* **14,** 127–143.

Lockner, D.A., Byerlee, J.D., Kuksenko, V., Ponomarev, A. & Sidorin, A. 1991. Quazi-static fault growth and shear fracture energy in granite, *Nature,* **350,** 39–42.

Lockner, D.A. & Moore, D.E., 1992. Microcrack interaction leading to shear fracture, in *Rock Mechanics*, pp. 807–814, eds Tillerson, J.R. & Wawersik, W.R., Balkema, Rotterdam.

Miannay, D.P., 1998. *Fracture Mechanics*, Springer-Verlag, New York.

Miannay, D.P., 2001. *Time-Dependent Fracture Mechanics*, Springer-Verlag, New York.

Scholz, C.H., Dawers, N.H., Yu, J.-Z. & Anders, M.H., 1993. Fault growth and Fault scaling laws: Preliminary results, *J. geophys. Res.,* **98**(B12), 21 951–21 961.

Sleep, N.H. & Blanpied, M.L., 1992. Creep, compaction and the weak rheology of major faults, *Nature,* **359,** 687–692.

Tang, C.A., 1997. Numerical simulation of progressive rock failure and associated seismicity, *Int. J. Rock Mech. Min. Sci.,* **34,** 249–262.

Tang, C.A. & Kaiser, P.K., 1998. Numerical simulation of cumulative damage and seismic energy release in unstable failure of brittle rock—Part 1, Fundamentals, *Int. J. Rock Mech. Min. Sci.,* **35,** 113–121.

Tang, C.A., Hudson, J.A. & Xu, X.H., 1993. *Rock Failure Instability and Related Aspects of Earthquake Mechanisms*, China Coal Industry Publishing House, Beijing.

Tang, C.A., Huang, M.L. & Zhao, X.D., 2003. Weak zone related seismic cycles in progressive failure leading to collapse in brittle crust, *Pure appl. Geophys.,* **160,** 2319–2328.

Vermilye, J.M. & Scholz, C.H., 1998. The process zone: A microstructural view of fault growth, *J. geophys. Res.,* **103**(B6), 12 223–12 237.